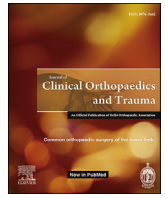




Contents lists available at ScienceDirect

## Journal of Clinical Orthopaedics and Trauma

journal homepage: [www.elsevier.com/locate/jcot](http://www.elsevier.com/locate/jcot)

## Multi-modality imaging approach to bone tumors - State-of-the art

Nidhi Goyal\*, Manas Kalra, Aditi Soni, Pankaj Baweja, Nitin P. Ghonghe

Indraprastha Apollo Hospital



## ARTICLE INFO

## Article history:

Received 1 April 2019

Received in revised form

28 May 2019

Accepted 28 May 2019

Available online 31 May 2019

## Keywords:

Bone tumors

Radiographs

X-rays

MRI (magnetic resonance imaging)

CT (computed tomography)

FDG PET/CT/MRI

Nuclear scan

## ABSTRACT

The approach to the radiographic diagnosis of bone tumors is much beyond the conventional radiographs in present era of multiplanar and functional imaging. Radiographs is still the most pertinent part of initial diagnosis of bone tumors, however, there are few limitations, like lesions in complex anatomy, marrow assessment, soft tissue resolution, which are important for staging. Diagnosis is just one aspect of the tumor evaluation, extent of marrow involvement by the tumor growth, involvement of overlying soft tissue, involvement of adjacent joint, and knowledge about skip lesions and metastasis are equally important for staging and treatment of the disease. Multimodality imaging like CT, MRI helps cover all these aspects. Emerging role of PETCT/PET MRI has further revolutionized the imaging of bone tumors by providing anatomical and morphological characteristics simultaneously and combining the whole body scan in same sitting.

This article will discuss the role of various imaging modalities along with illustrative examples of few cases. Team work between radiologist with orthopedic oncologist and pathologist will help in deciding a road map for diagnosing and treatment of bone tumors. Follow up scanning with MRI and PET FDG scan has also been well established in assessing therapeutic response.

© 2019 Delhi Orthopedic Association. All rights reserved.

## 1. Introduction

Primary bone tumours encompass aggressive and non-aggressive lesions of varying morphology and tissue origin. This article emphasises on radiological appearance of bone tumours according to the radiographic characteristics and features. Radiography remains the mainstay for initial diagnosis and other advanced imaging modalities being useful in evaluating the extent of lesion and its local and distant staging for the appropriate treatment and in assessing therapeutic response. Choice of imaging modalities had been discussed tailored around the disease process with the specific advantages of each modality in entire diagnosis and treatment part. A review with illustrative examples of varied variety of cases has been presented.

## 2. Imaging technique to evaluate bone tumor

## 2.1. Evaluation of the bone lesion

Radiologist plays an important role in initial diagnosis, work up

and staging of bone tumors and subsequently in deciding the management of the tumors. The diagnostic work up of the bone tumors often requires multimodality approach, ranging from radiography, to CT, MRI, bone scintigraphy and PETCT/PETMRI. Every modality contributes differently in the evaluation of bone tumors and in varying combinations customized to the disease process under evaluation will provide a precise road map for the radiographic diagnosis and management of bone tumors.

## 2.1.1. Radiography

Radiographs are performed for any clinical symptoms of bone pain or swelling and the x-rays are preferably obtained in two planes AP and Lateral/oblique. Conventional radiography is the initial imaging modality and is the most optimal way to evaluate the primary bone tumors.<sup>1,2</sup> Its relatively inexpensive and unique advantage of 2D image allows characterization of the lesion based on the features seen on radiographs. The information of site of lesion in bone, along with imaging characteristics of tumor including margin and edges of the lesion, matrix mineralization, cortical involvement and periosteal reaction all can be seen on plain radiography.<sup>3</sup> Radiographs are thus the mainstay for initial diagnosis in most cases and cornerstone for differential diagnosis.<sup>4</sup>

A deficit of conventional radiography is with lesions which are located in complex anatomical locations, like in spine, iliac bones and in posterior elements of vertebrae where overlapping of

\* Corresponding author.

E-mail addresses: [Nidhi.i.goyal@gmail.com](mailto:Nidhi.i.goyal@gmail.com) (N. Goyal), [Manaskalra27@gmail.com](mailto:Manaskalra27@gmail.com) (M. Kalra), [Aditisoni1979@gmail.com](mailto:Aditisoni1979@gmail.com) (A. Soni), [drpankajbaweja@gmail.com](mailto:drpankajbaweja@gmail.com) (P. Baweja).



**Fig. 1a.** X-ray (a) AP (b) lateral reveals a large aggressive lesion in proximal tibia with resorption of overlying cortex and overlying soft tissue swelling: Ewing's sarcoma. (\*) Depicts permeative pattern of destruction (arrow) showing ill defined margin with broad zone of transition. MRI (c) T2 FAT SAT (d) T1W coronal, (e) Post contrast coronal and sagittal T1W Images reveal heterogeneously enhancing mass lesion in proximal tibia with extension into overlying soft tissue. There is involvement of the epiphysis and articular margin of tibia and extension into knee joint. DWI (f) images show restriction in the soft tissue with reversal of signal on ADC (g). (h) CT in coronal planes shows tibial erosion with extra osseous soft tissue and no mineralization.

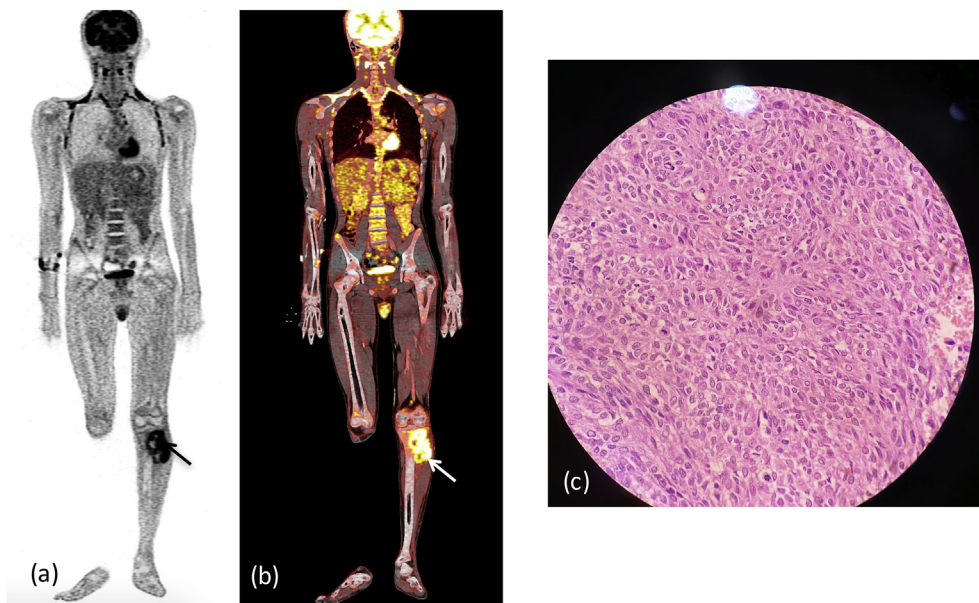


**Fig. 1b.** (a), (b) FDG/PET CT revealing intense FDG activity within the lesion (arrow).

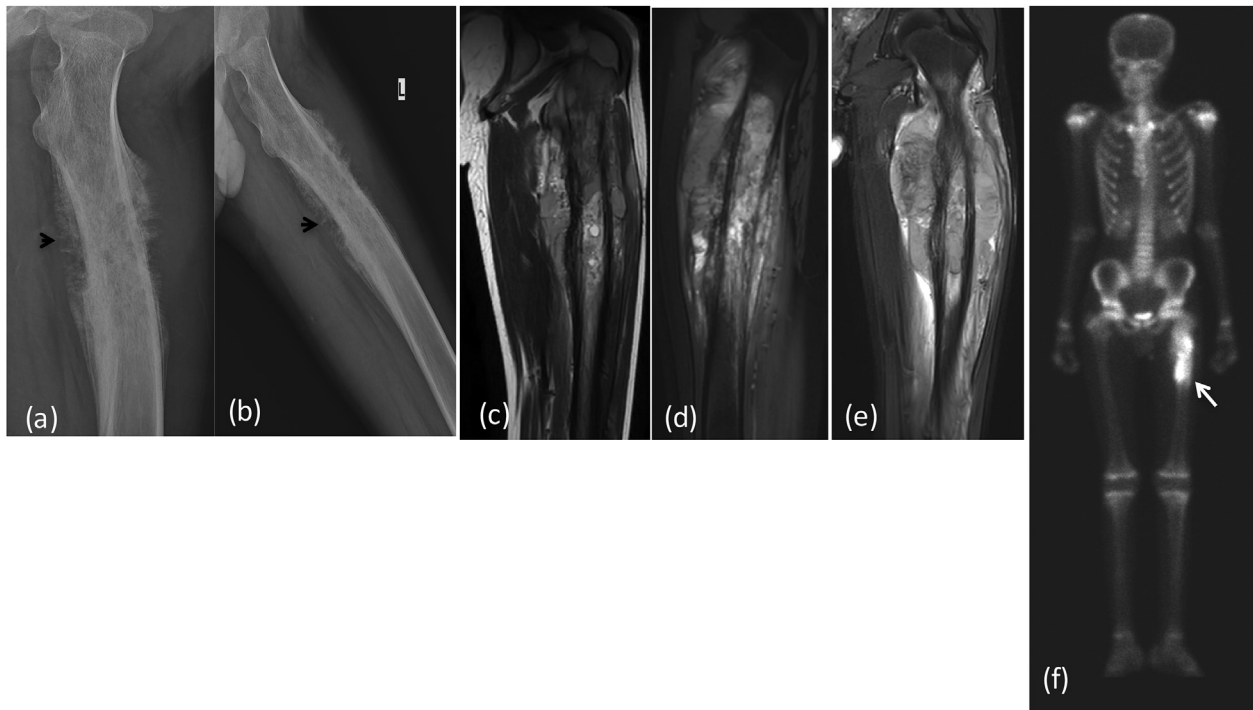


**Fig. 2a.** X-ray (a) lateral (b) oblique reveals a permeative pattern of destruction with ill defined margins in proximal femoral shaft with resorption of overlying cortex.: Ewing's sarcoma. (arrowhead) depicts interrupted, & (arrow) showing multilaminated periosteal reaction. MRI (c) T2W coronal (d) T2W FAT SAT sagittal, (e) Post contrast coronal T1W Images reveal heterogeneous enhancing mass lesion in proximal tibia with extension into overlying soft tissue involving cortex. (f) Nuclear scan revealing intense uptake within the lesion (arrow). (c) Microscopic histopathology smear showing sheets of round cells.

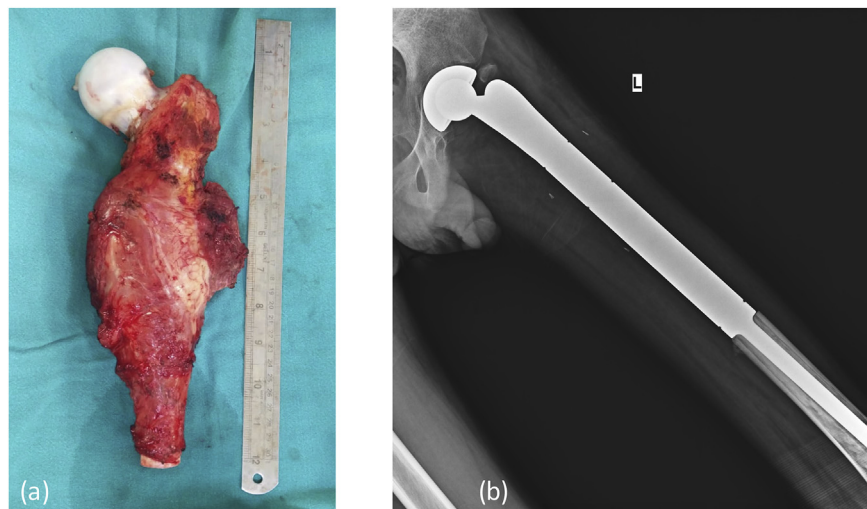


**Fig. 2b.** (a) Gross histopathology specimen of the excised bone containing the tumor.

structures on 2D planes limits the evaluation. The evaluations of soft tissue along with precise extent of medullary involvement are other limitations.

### 2.1.2. CT scan

Multidetector CT allows precise anatomical delineation and evaluation of the lesions in complex anatomical location, where radiographs are not sufficient due to limited contrast resolution.<sup>5</sup> Visualization of minor bony changes, small calcifications, tumor mineralization, cortical changes and periosteal reactions are best seen on CT scans.<sup>5</sup> Isotropic imaging with latest 16 slices and above

CT scanners provides excellent 3D evaluation of lesion and bone and also provides images in all planes, which can be used for accurate measurements required for the surgery. Along with tumor evaluation, staging of tumor through abdominal or chest CT remains the fundamental protocol.<sup>6</sup>

The lack of characterization of soft tissue along with lack of precise extent of medullary involvement are major limitations for precise delineation of the lesion extent.

### 2.1.3. Nuclear scan

A bone scan has excellent sensitivity for assessing bony changes

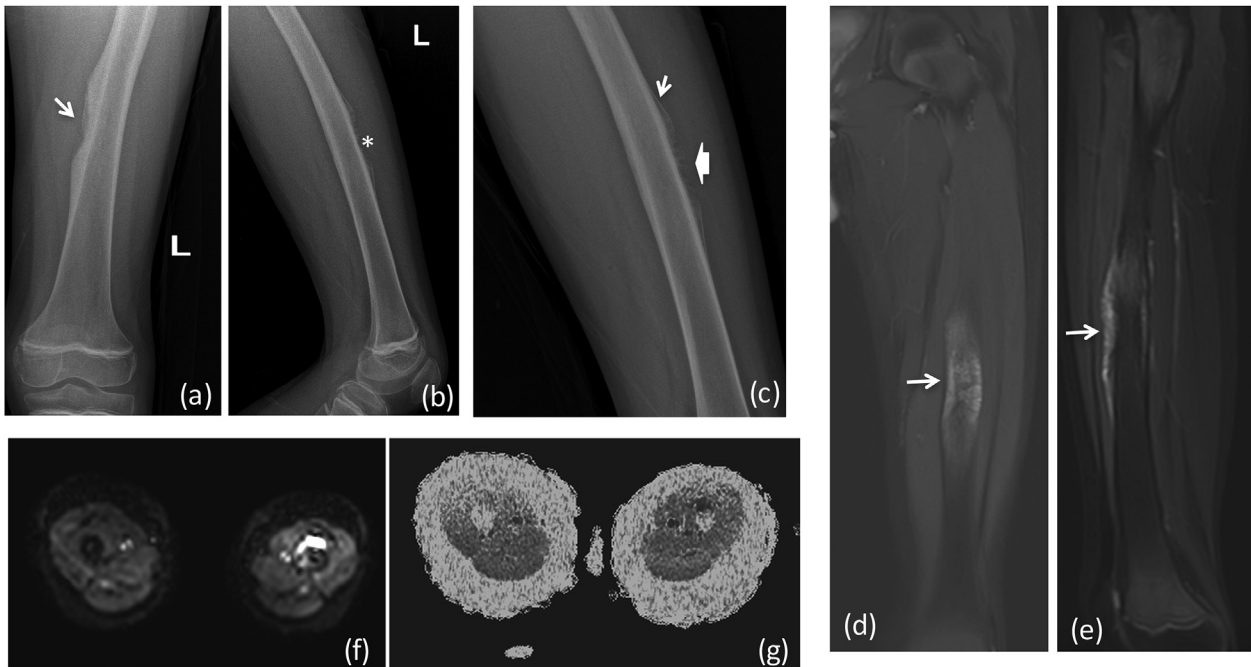


**Fig. 3a.** X-ray (a) AP (b) lateral and (c) oblique reveals a cortical irregularity (arrow) with aggressive periosteal reaction along the antero-medial aspect of mid shaft of left femur: Ewing's sarcoma. There is sunray (\*), and multilaminated (arrowhead) types of periosteal reaction. Also seen in Codman's triangle (arrow) in (c). MRI (d) T2 FAT SAT coronal, (e) sagittal Images reveal aggressive periosteal reaction with ill defined marrow edema in mid femur with extension into overlying soft tissue. DWI (f) images show restriction in the lesion with reversal of signal on ADC (g). (b) Post operative X-Ray showing post tumor resection Endoprosthesis in situ.

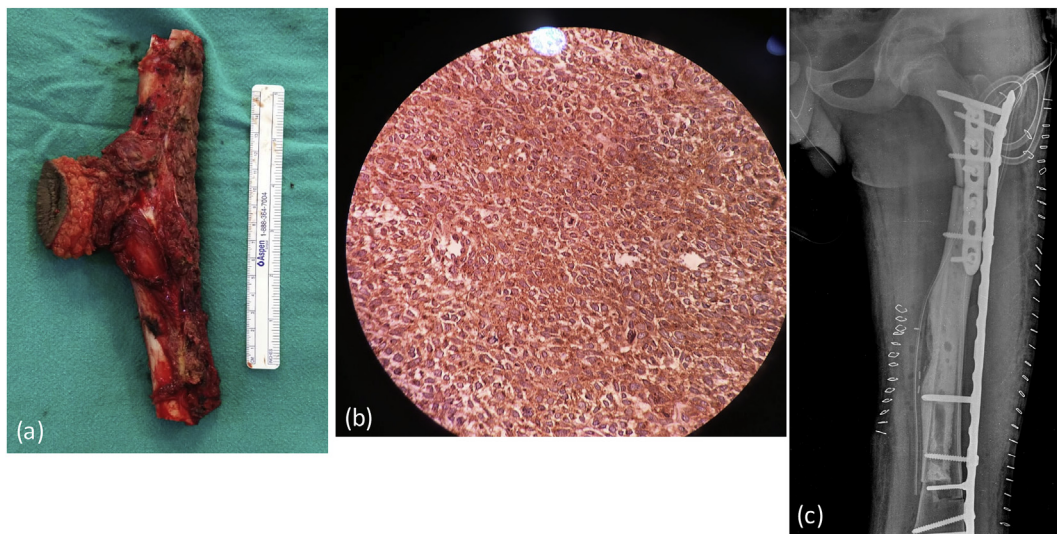


**Fig. 3b.** (a) Gross histopathology specimen of the excised bone containing the tumor. (b) Microscopic histopathology smear showing sheets of round cells. (c): Post extracorporeal radiotherapy - X-Ray showing reimplanted bony graft in situ.

and is irreplaceable as screening tool for the primary lesion and distant bony metastasis. Therefore, the conditions, which may not be evident on other images, can be detected with nuclear imaging. It's a best tool to assess the cause of pain, by doing screening test for the entire skeleton, when the cause of the pain cannot be localized, Protocols may vary, but standardized technique is to acquire images 2–6 h after intravenous administration of 740–925 MBq of Tc-99m-labeled diphosphanates.<sup>7</sup> The images are acquired once the tracer is washed out of the soft tissue and persisting in bone thus improved visualization of the bones. Images are acquired of the whole body in both anterior and posterior projections and additional images are taken if required.

#### 2.1.4. MRI

MRI is considered the best tool for local staging of bone tumors. The inherent capability of soft tissue characterization and visualization of bone marrow by MRI remains the mainstay for evaluation of suspected or diagnosed bone tumor. Tumor contents and hence characterization of bone tumors on basis of tissue composition can be done on MRI along with precise depiction of bone marrow and soft tissue involvement.

If the patient continues to have symptoms and radiographs do not show any abnormality, additional imaging is recommended. Lytic bone lesions can be seen on plain radiographs only when there is more than 30–50% loss of mineralization.<sup>8</sup> Therefore MRI is

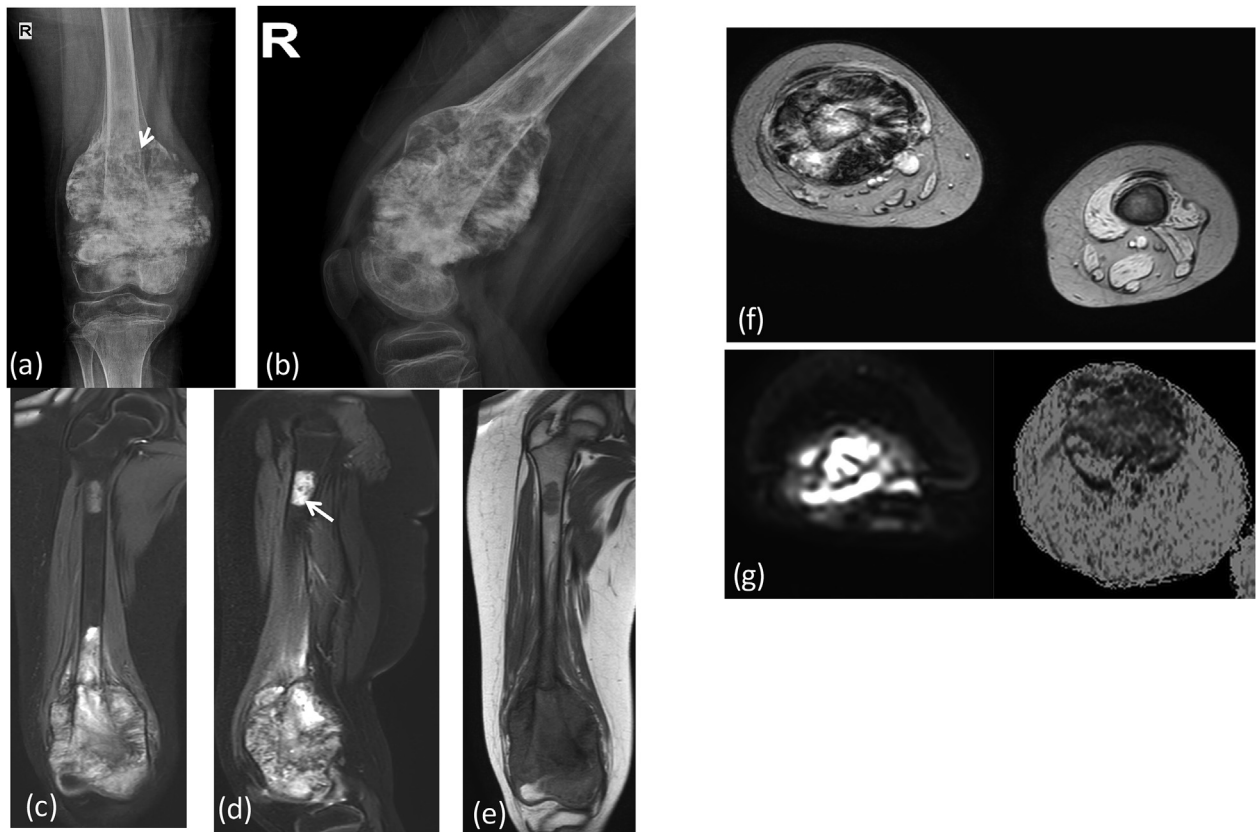


**Fig. 4a.** X-ray (a) AP (b) lateral shows expansile mixed lytic and sclerotic lesion in lower meta-diaphyses of femur with a broad zone of transition, (arrow) showing Codman's triangle. There is cumulus cloud formation: Osteosarcoma. MRI (c & d) T2 FAT SAT coronal, (e) coronal T1W reveal mixed intensity mass lesion in distal femur with extension into overlying soft tissue, (f) SWI Images showing areas of blooming. There is involvement of the epiphysis and articular margin of femur. Skip lesion is seen in proximal femur upper shaft (arrow). DWI & ADC (g) images show restriction in the soft tissue with reversal of signal on ADC.

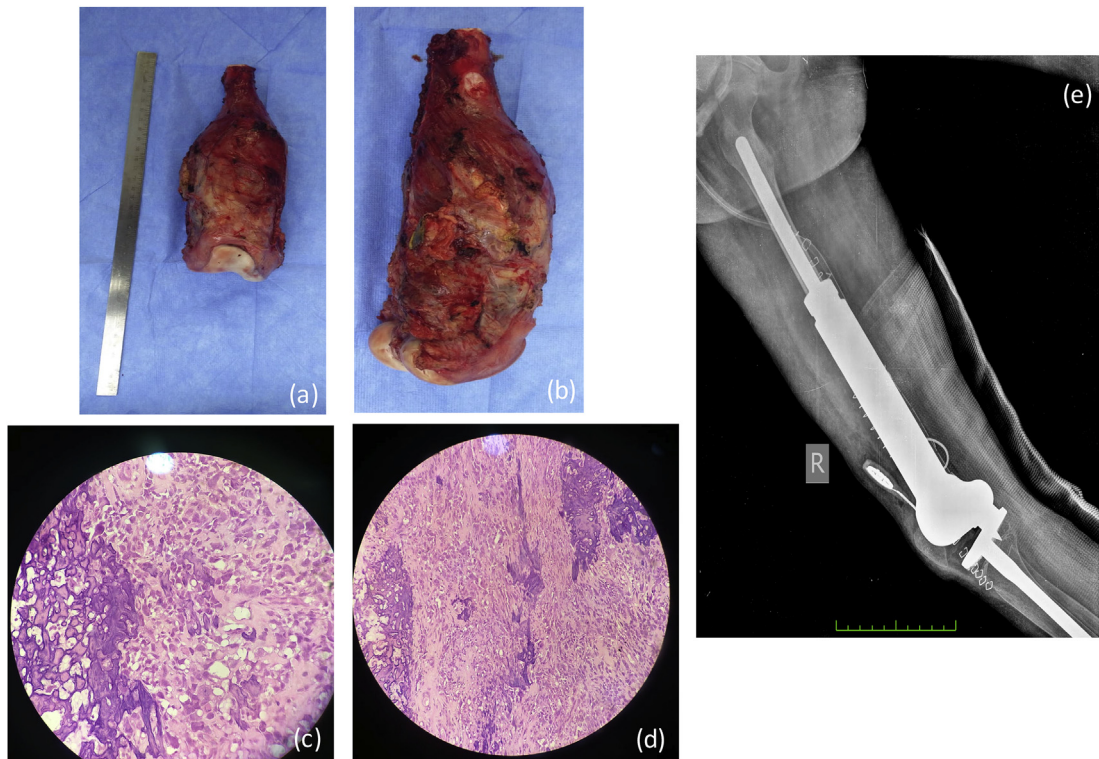


**Fig. 4b.** (a & b) Gross histopathology specimen of the excised bone containing the tumor. (c & d) Microscopic histopathology sarcomatous tumor cells with osteoblasts predominance showing nuclear atypia. (e) Post operative X-Ray showing post tumor resection Endoprosthesis in situ.

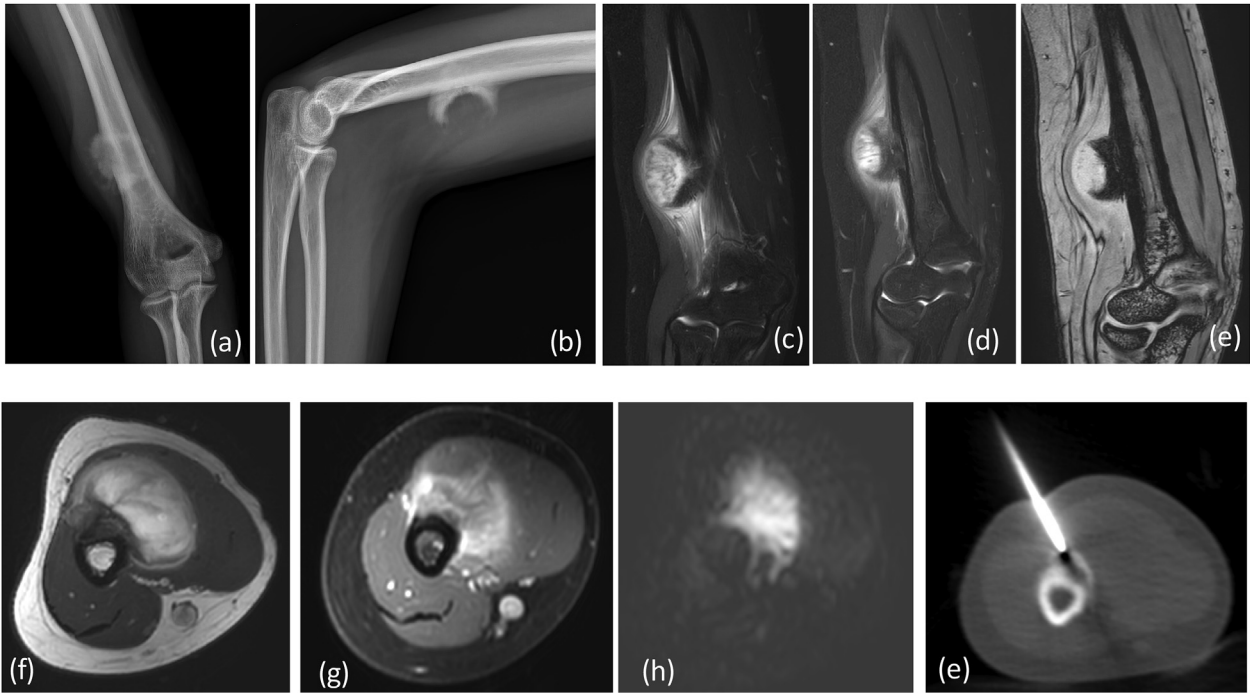


**Fig. 5.** X-ray (a) AP (b) lateral shows saucerization of the cortex, and lobulated and ossified exophytic mass lesion with cortical thickening with codman's triangle seen at margin of the lesion. MRI (c & d) T2 FAT SAT, (e) SWI coronal and axial T2W (f), post contrast T1W (g) showing large lobulated mass lesion displaying ossified matrix, appearing low signal on all sequences. The lesion is arising from the cortex, with large enhancing soft tissue mass lesion. DWI images (h) reveal restricted diffusion within the lesion. CT (e) images reveals dense ossified matrix and CT guided Biopsy needle is seen.

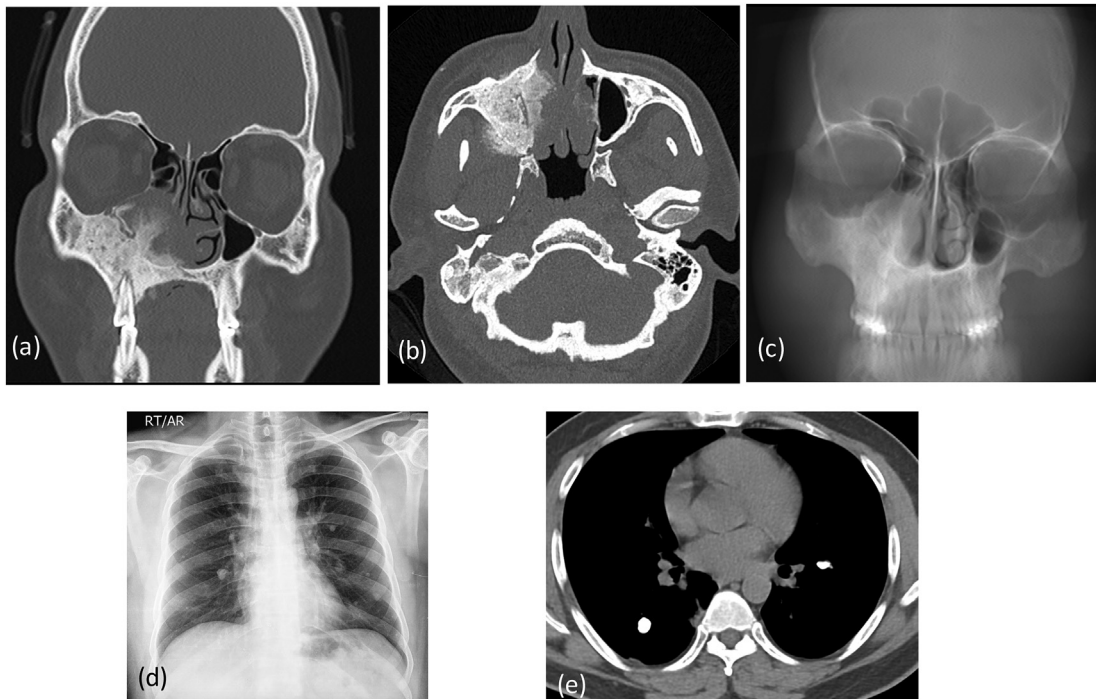


**Fig. 6a.** CT coronal (a) axial images (b) show large new bone formation with cortical thickening and aggressive periosteal reaction involving walls of right maxillary sinus. MIP mean image<sup>®</sup> of the face is showing thickening and sclerosis of right maxillary bone. X-ray chest (d) shows few calcified lesions in both the lungs. Axial sections of CT (e) chest confirmed multiple nodular calcified lesions: metastasis.

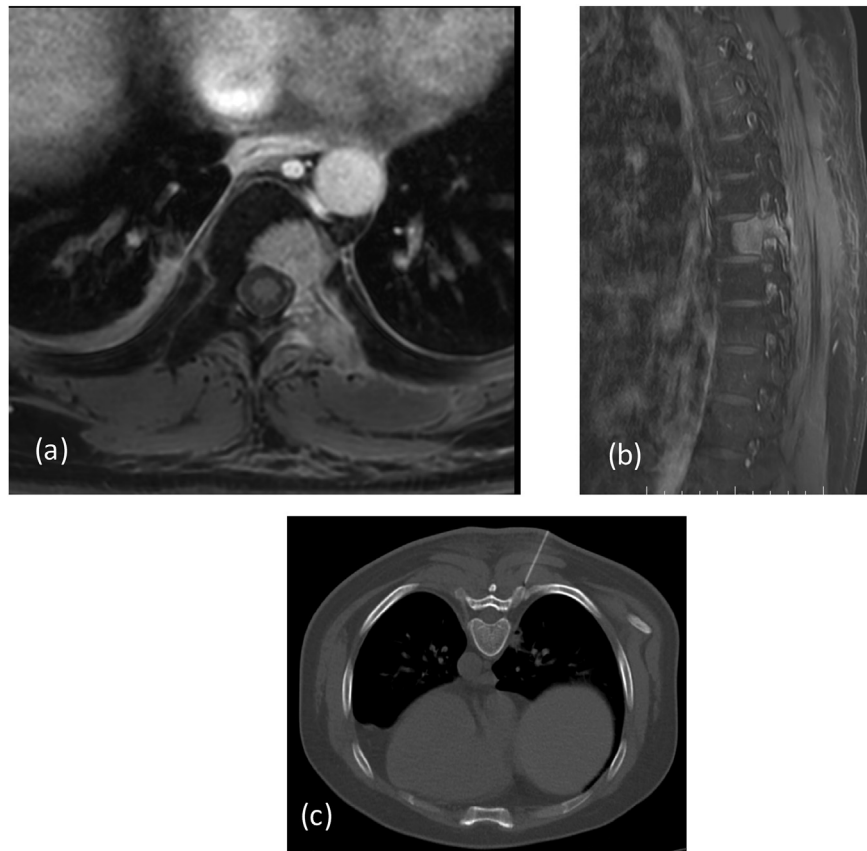


**Fig. 6b.** MRI in axial (a) and sagittal (b) planes reveals metastasis along posterior body and elements of D8 vertebrae. There is a significant soft tissue extending outside the bony margins. CT guided Biopsy (c): Biopsy needle is seen.

the preferred modality in these cases to assess bone marrow. MRI should be interpreted only with concurrent radiographs.<sup>9</sup>

Newer state of the art imaging techniques compiled under functional MRI includes dynamic contrast enhanced imaging (Perfusion MRI), Diffusion Weighted Imaging (DWI) and MR Spectroscopy. Functional Magnetic resonance imaging has added advantages over structural MRI, in tissue characterisation and in staging of bone tumours.

Standard MRI helps to evaluate the structural changes in bones and extent of the disease, and the morphology of the tumor is better assessed by DWI and perfusion MRI which also helps in differentiating benign from malignant etiology. The evaluation of tissue cellularity and presence of viable tissue or necrosis which are criteria to assess follow up post chemotherapy can not be determined by standard MRI, where perfusion MRI and DWI plays an important role.

Perfusion imaging representing dynamic contrast imaging is the acquisition of data post contrast enhancement, acquiring multiple sets of data through the specified diseased segment. The enhancement pattern is then plotted against time curve and early enhancement is evaluated representing the vascularisation and perfusion and hence viability of tissue within the tumour. Dynamic MRI, therefore helps to guide biopsy site by delineating the viable tumour location and monitoring the changes post chemotherapy by differentiating fibrous tissue/scarring/necrosis from viable tissue.<sup>23–25</sup>

DWI adds on functional information over the structural evaluation by providing qualitative assessment of the tissue cellularity. Tumours differ in the cellular structure with malignant tumours being more cellular displaying restricted diffusion. Diffusion

weighted images show restricted diffusion and reversal of signal on ADC (apparent diffusion coefficient) of the tissue which are highly cellular and resultant has less Brownian movement, the principle behind DWI.<sup>26,27</sup>

#### 2.1.5. Monitoring the treatment response

Treatment response is monitored by multimodality approach, primarily by X-Rays and MRI. Standard MRI protocols provide a composite outlook of the tumor response to treatment. However in the cases where there is no obvious decrease or increase in the size of lesion the viability of the tissue will help to evaluate the treatment response. This information to some extent can be interpreted from standard MRI, and the functional MRI is used as an adjunctive imaging modality complementing morphological imaging.

In bone tumours, the dynamic contrast scans showing early and rapidly progressive enhancement indicates residual or recurrent tumour, whereas absence of early enhancement indicates a good response. Similarly DWI with ADC calculation helps to differentiate viable from non-viable component of the tissue, demonstrating restricted diffusion in residual tumour.

#### 2.1.6. PET CT/PET MRI

FDG PET scans provides a noninvasive method to assess the aggressiveness of tumor. It's a one-stop solution for staging the tumor and to rule out distant bony and soft tissue (liver or lung or lymph nodal) metastasis. It's again a useful technique to assess the skip lesions in equivocal conditions.<sup>10</sup>

Bone lesions frequently seen in F<sup>18</sup>FDG PET/CT are FDG avid. FDG uptake in a bone lesion does not decide the morphologic features of lesion and hence does not characterize the bone tumor. FDG avidity

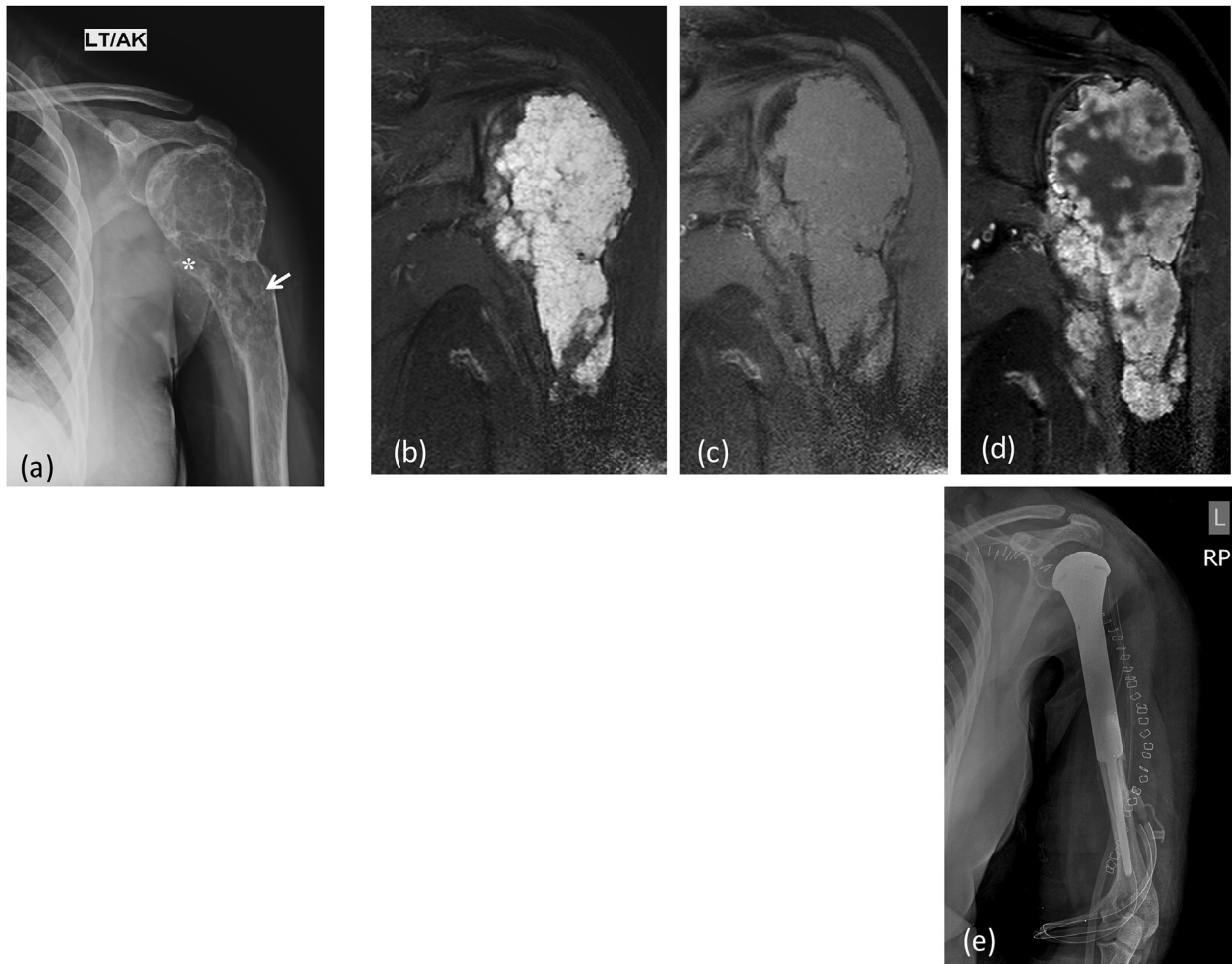


**Fig. 7.** X-ray (a) AP view of right humerus: an aggressive bone lesion in proximal shaft with cortical irregularity\* and few specks of calcifications within the central septated matrix (arrow). MRI (b) T2 FAT SAT (c) T1W coronal. (d) Post contrast coronal T1W Images reveal heterogeneous enhancing mass lesion in proximal humerus with extension into overlying soft tissue. There is involvement of the epiphysis. Note the intense bright signal of chondroid matrix on T2 weighted images. Post operative X-Ray (e) showing post tumor resection Endoprosthesis in situ.

and morphology of the tumor are independent factors and together are important in staging the tumor and determining the treatment response. Morphological features are seen best on radiographs or CT done as preliminary part of FDG scan. Once a primary diagnosis of the bone tumor has been made, like that of Ewing's or Osteosarcoma, PET scan of the whole body is done for staging and also for evaluation of therapeutic response.

FDG avidity of the lesion decides the aggressiveness of the lesion with malignant lesion being more avid than the benign bone lesions of same histological types.<sup>11,12</sup>

FDG PET/MRI is another emerging imaging modality, which results in reduced radiation with increased anatomical resolution. PET/MRI has been proven superior to PET/CT in evaluation of brain, soft tissue component of the lesions and also in bone marrow evaluation.<sup>13,14</sup>

### 3. Image guided biopsies

Histopathological evaluation of specimen drawn from the bone tumor under image guidance is the final step in diagnosis and grading of the tumor. Radiologist have a major role to play in image guided biopsies of the tumor, which should be performed after all the diagnostic evaluation has been done as the post biopsy changes

can alter the radiological appearance of the lesion. The track for the biopsy should be well planned in collaboration with the surgeon to include the biopsy track within the surgical bed.<sup>15</sup>

#### 3.1. Imaging features

A patient with bone tumor, seeks medical advice when it's painful, associated with a mass, or a fracture or is detected incidentally on x-ray. The Appropriateness Criteria<sup>9</sup> by American college of Radiology dictates that the first line of investigation for initial evaluation of bone tumors should be a radiograph.

Primary bone lesions seen by radiologists have specific radiographic characteristics, which help them to be classified as aggressive and non-aggressive lesions. The margin of the lesion, zone of transition, cortical expansion, and periosteal reaction and matrix mineralization are the features, which decide the nature of the bone tumor.

Margins and zone of transition of the bone tumor defines the growth rate of the lesion, and has been classified in three types.<sup>16–18</sup> Type I are geographic lesions and has three further variants with 1A lesions having well defined borders with sclerotic margins, (Fig. 11B), type 1B including the lesions without sclerotic margins and narrow zone of transition and type 1C have ill defined



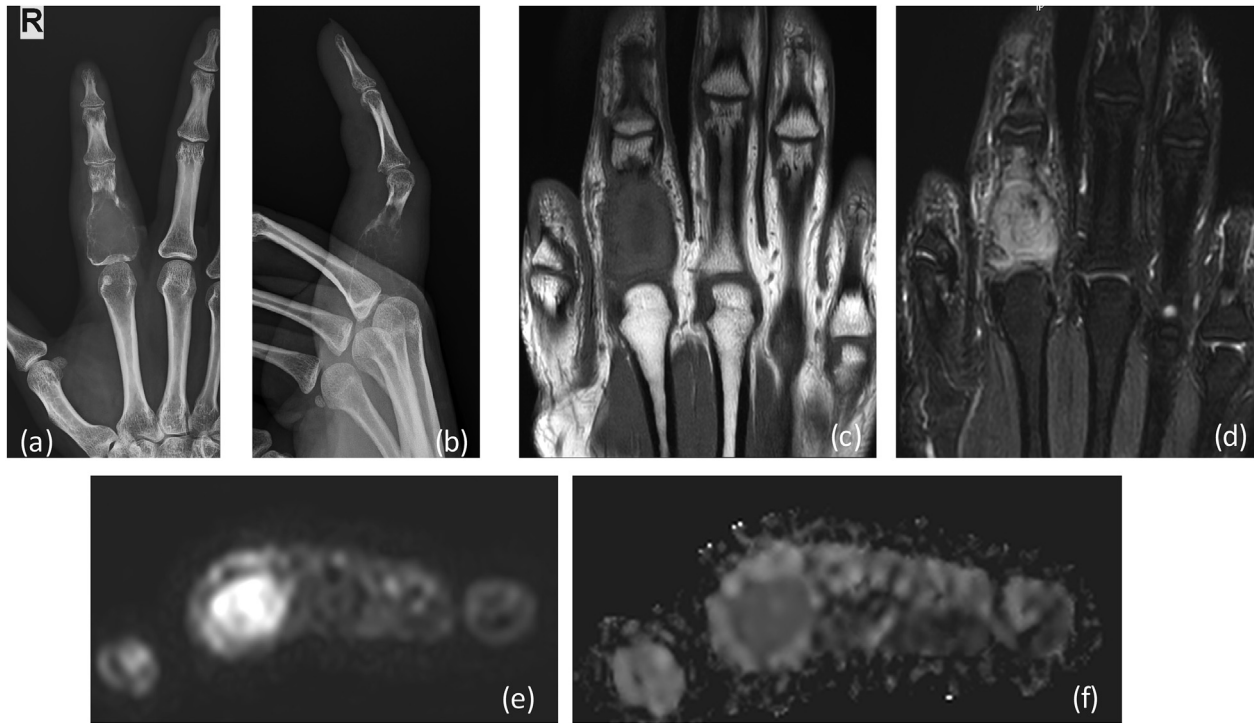


**Fig. 8a.** X-ray (a) AP (b) lateral reveals a large expansile lytic lesion on in proximal shaft of proximal phalanx of 4th finger extending up to the articular margin: GCT. No matrix mineralization noted. MRI (c) T1W coronal, (d) T2 FAT SAT Images reveal heterogenous intensity mass lesion in proximal phalanx with thinning of overlying cortex. DWI (e) images show restriction in the soft tissue with reversal of signal on ADC (f).

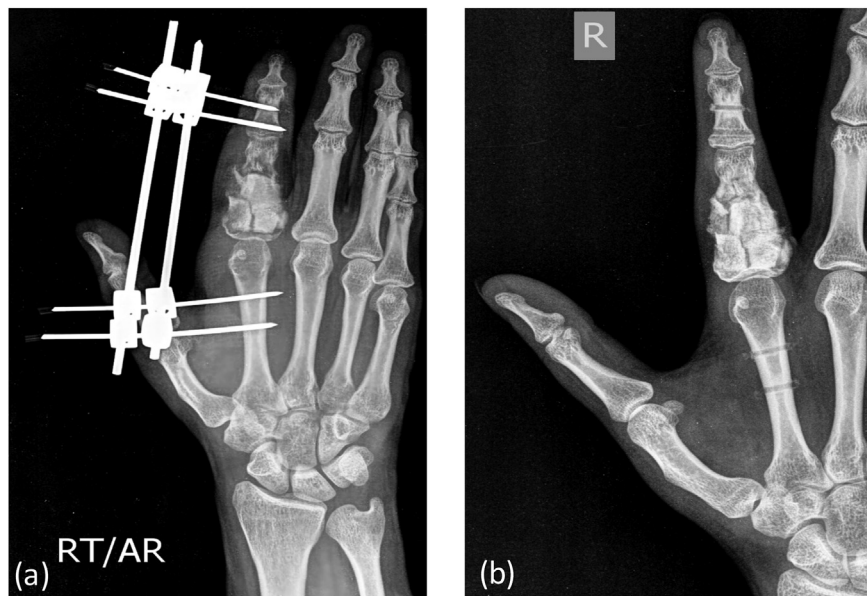


**Fig. 8b.** Post operative X-Ray showing (b) bone grafting/cementing at the site of tumor resection with (a) external fixator in situ.

margins. Non geographical lesions have broad zone of transition and have either type II or III margins, with moth eaten pattern of destruction being Type II and permeative pattern being type III (Fig. 2A).

Matrix mineralization decides the morphology of the lesion like, osteoid, chondroid or fibrous lesions.<sup>19</sup>

Periosteal reaction represents the growth potential of the bone tumor<sup>20</sup> and helps to differentiate aggressive from non-aggressive

bone lesions. Solid periosteal reaction or periostitis is indicator of slow growing pattern of the underlying bone lesion. Multi-lamellated periosteal reaction also termed as onionskin appearance depicts intermittent aggressive growth pattern commonly seen in Ewing's sarcoma. Interrupted type of periosteal reaction gives a sunburst pattern or spiculated appearance is seen in most aggressive tumors, suggesting malignancy like osteosarcoma or Ewing's sarcoma. (Fig. 2A). Extra osseous growing mass lesion may elevate

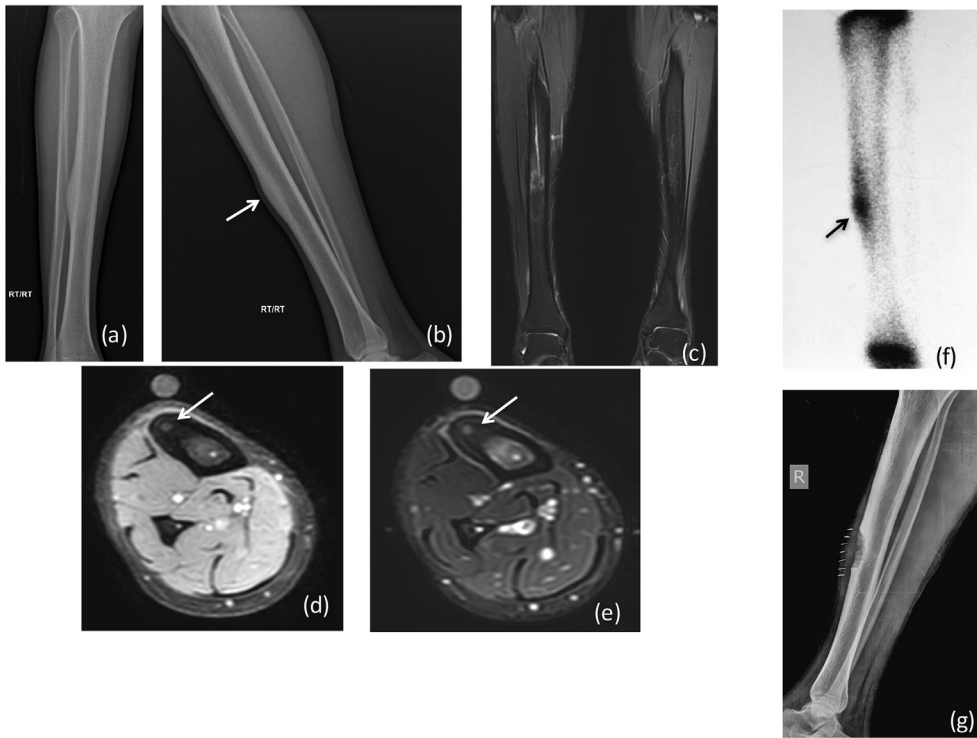


**Fig. 9.** Radiographs (a) AP and (b) lateral X-ray show increased cortical thickness involving the mid tibial shaft on the lateral aspect, and there is associated sclerosis. MRI (c) T2 FAT SAT coronal & (d) T1w (e) T2W axial Images showing extensive bone marrow edema, with a nidus (arrow) demonstrated within the cortex and resultant cortical thickening: Osteoid Nuclear scan (f) revealing intense uptake within the lesion (arrow). Post operative X-Ray (g) showing defect of en-bloc excision at the site of tumor.

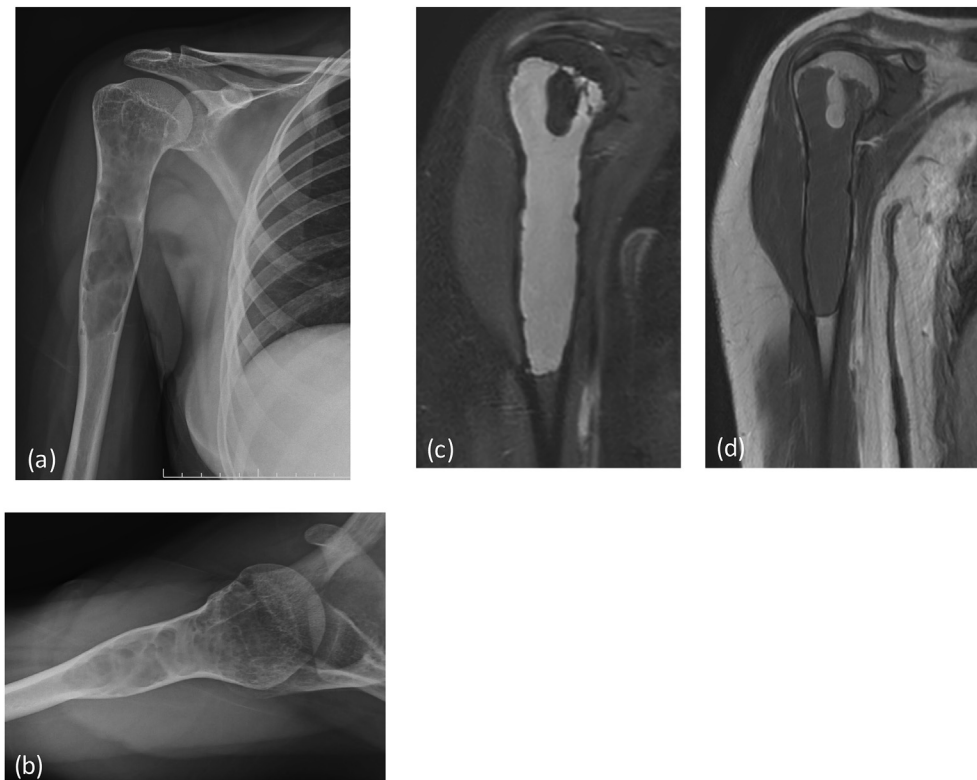


**Fig. 10.** X-ray (a) AP (b) lateral reveals a large eccentric expansile lytic lesion in the proximal meta-diaphysis of the right humerus. It has multiple internal septations, cortical thinning, with narrow zone of transition. MRI (c) T2W FAT SAT (d) T1W coronal images reveals a large cystic lesion in proximal humerus confirming the diagnosis of benign bony cystic lesion: simple bone cyst.

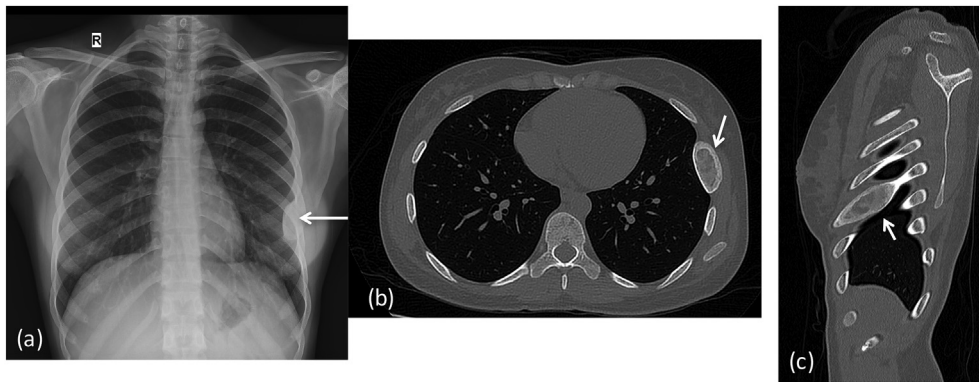


**Fig. 11.** X-ray (a) Chest expansion of lateral aspect of left 6th rib, with predominant sclerotic appearance. CT chest (b) axial & (c) sagittal images shows a well circumscribed expansile lytic lesion in left 6th rib with sclerotic margins and ground glass matrix (arrows): Fibrous dysplasia.



**Fig. 12.** Radiograph (a) AP (b) lateral of knee joint reveals a bony outgrowth (\*) from posterior aspect of the tibia pointing away from the joint.

periosteum from the underlying cortex, giving a triangular interface referred as Codman's triangle. (Fig. 3A(c)).

Non-aggressive lesions include a narrow zone of transition between the lesion and adjacent parent bone, thickening or thinning of the cortex without resorption/erosion, mature periostitis, and lack of soft tissue component. Aggressive lesions on radiographs have ill defined margins seen as a wide zone of transition with adjacent parent bone, cortical resorption/erosions, interrupted periosteal reaction showing new bone formation (onion skin or sunray type of periosteal reaction) and associated soft tissue mass.

### 3.1.1. Staging of primary bone tumor

Benign lesions: Enneking<sup>21</sup> categorised latent benign tumors as stage I and these are usually “no touch lesions” which remains

unchanged or may heal spontaneously e.g., non ossifying fibroma, or focal cortical defect. These lesions should be left untouched. Stage 2 tumours are actively growing tumors with radiological benign features and growth is limited within anatomical boundaries, e.g. fibrous tumor (Fig. 11A and B), simple bone cyst (Fig. 10A) or chondroblastoma. These tumours are treated with curettage and bone grafting. MRI precisely delineates the extension of disease in the marrow. Stage 3 are benign bone tumours with locally invasive behaviour e.g., giant cell tumor (Fig. 8). MRI is helpful to assess the extension of the disease process. There was surgical excision of the tumour with curettage and bone grafting with or without adjuvant therapy. Few cases are illustrated in Table 1 depicting clinical history, radiological evaluation and follow up. Figures of the cases are mentioned within the table.

**Table 1**  
Few illustrated cases with clinical profile, radiological findings and follow up.

Case	Clinical	Imaging	Management
1.	<p>8-year boy: gradually increasing, painful lower leg swelling.</p> <p><b>Examination</b> showed tender, well defined swelling in infrapatellar region along the region of tibial condyle. advised.</p>	<p><b>AP and lateral X rays</b> of the knee joint showed:</p> <ul style="list-style-type: none"> <li>• Ill defined lytic lesion with permeative bone destruction involving the proximal metadiaphysis of tibia along the tibial tubercle with a broad zone of transition and varying types of periosteal reaction.</li> <li>• Resorption of overlying cortex with displaced soft tissue planes.</li> <li>• No definite matrix mineralization seen.(Fig. 1A)</li> </ul> <p><b>Diagnosis:</b> Aggressive lesion: Ewing's Sarcoma</p> <p><b>MRI of the knee</b></p> <ul style="list-style-type: none"> <li>• T2 W and PD FAT SAT: hyperintense mixed intensity soft tissue lesion involving the proximal diaphysis of tibia, and marrow infiltration is extending. upto the proximal one-third of the tibial shaft. There is extra-osseous extension of the mass lesion involving the muscles with extension till the subcutaneous plane and stretching of overlying skin.</li> <li>• Post contrast scans revealed heterogeneous enhancement of the mass lesion with early wash out of the contrast.</li> <li>• DWI images reveal diffusion restriction with ADC reversal confirming the malignant nature of the lesion (Fig. 1A).</li> </ul> <p>The lesion is involving the epiphysis, reaching unto the cortex and likely involving articular margin and cartilage with involvement of distal part of patellar tendon.</p> <p><b>PET CT</b> revealed:</p> <ul style="list-style-type: none"> <li>• Strong FDG avidity in the lesion with no abnormal uptake in the rest of the tibia and proximal and distal joints or anywhere else in the body ruling out distant metastases. Lungs and liver were free of any metastasis (Fig. 1B).</li> </ul>	<p><b>Biopsy:</b> Ewing's sarcoma grade 3 (Fig. 1B).</p> <p><b>Treatment:</b> Post chemotherapy surgery Wide resection and reconstruction by endoprosthesis and knee joint replacement.</p>
2.	<p>15-year- boy: pain in left thigh region, gradually increasing in intensity.</p> <p><b>Examinations:</b> vague swelling and diffuse tenderness in the proximal thigh region on left side.</p>	<p><b>AP and lateral X ray</b> of the knee joint:</p> <ul style="list-style-type: none"> <li>• Permeative pattern of destruction in the proximal shaft of left femur involving metadiaphysis with a broad zone of transition.</li> <li>• Overlying cortex is ill defined with mixed sunray and onion peel type of periosteal reaction with presence of Codman's triangle and effaced/displaced overlying fat planes.</li> <li>• No definite matrix mineralization (Fig. 2A).</li> </ul> <p><b>Diagnosis:</b> Appearance represents aggressive bone tumor with Ewing's sarcoma kept as principle diagnosis with other remote possibility of osteosarcoma.</p> <p><b>MRI of the left femur:</b></p> <ul style="list-style-type: none"> <li>• heterogeneously enhancing soft tissue mass lesion involving the proximal diaphysis of femur with early enhancement in dynamic scans.</li> <li>• There is extra-osseous extension of the mass lesion involving mainly the vastus group of muscles and relative sparing of posterior compartment.</li> <li>• DWI images reveal diffusion restriction with ADC reversal confirming the highly cellular nature of the lesion (Fig. 2A).</li> </ul> <p><b>Radionuclide bone imaging:</b></p> <ul style="list-style-type: none"> <li>• Diffuse uptake in the lesion with no abnormal uptake in the rest body ruling out distant bony metastases or lung metastasis (Fig. 2A).</li> </ul>	<p><b>Biopsy:</b> confirmed the diagnosis of Ewing's sarcoma.</p> <p><b>Treatment:</b></p> <ul style="list-style-type: none"> <li>• adjuvant chemotherapy followed by wide resection and reconstruction by endoprosthesis including left hip prosthesis was done (Fig. 2B).</li> <li>• The margin of the removed part of the bone was free of disease and the patient is followed on adjuvant chemotherapy</li> </ul>
3.	<p>13-year- boy: pain in left mid thigh region with diffuse tenderness in the mid thigh region.</p> <p><b>Examination</b> revealed diffuse tenderness in the mid thigh region. X ray of the left thigh was advised.</p>	<p><b>AP and lateral X rays</b> of the femur:</p> <ul style="list-style-type: none"> <li>• cortical irregularity with aggressive periosteal reaction along the antero-medial aspect of mid shaft of left femur (Fig. 3A).</li> </ul> <p><b>Diagnosis:</b> Possibility of aggressive bone lesion and MRI done for further evaluation.</p> <p><b>MRI of the left femur</b> including the knee joint:</p> <ul style="list-style-type: none"> <li>• cortical thinning and irregularity along the antero-medial aspect of mid diaphysis of femur with diffuse and interrupted periosteal reaction and adjacent marrow edema. No obvious involvement of overlying thigh muscles (Fig. 3A) was seen.</li> <li>• DWI imaged reveals diffusion restriction with ADC reversal within the lesion.</li> <li>• Possibility of Ewing's sarcoma was kept, radiologically.</li> </ul> <p><b>Chest X-ray</b> was done which was within normal limits.</p>	<p><b>Biopsy:</b> Ewing's Sarcoma.</p> <p><b>Treatment:</b></p> <ul style="list-style-type: none"> <li>• Euro Ewing's protocol: extracorporeal Radiotherapy to the involved area (Fig. 3B).</li> <li>• The bone containing the tumor excised, and was subjected to single high dose of radiotherapy.</li> <li>• The treated bone replanted followed by adjuvant chemotherapy to the patient.</li> <li>• Post replant surgery X-rays were done (Fig. 3B) maintaining adjuvant chemotherapy.</li> </ul>

Table 1 (continued)

Case	Clinical	Imaging	Management
4.	9-year male: history of pain and swelling in the right knee joint. <b>Clinical examination</b> showed a swelling in the lower end of the thigh with restricted movement at the knee. X ray of the right femur with knee joint was advised.	<b>X ray of femur with knee:</b> <ul style="list-style-type: none"> <li>an expansile mixed lytic and sclerotic lesion involving lower end of the right femur with broad zone of transition and resorption of the overlying cortex and aggressive periosteal reaction (Fig. 4A). There is extra-osseous extension of the lesion and new bone formation in the overlying soft tissue resulting in cumulus cloud formation.</li> </ul> <p><b>Diagnosis:</b> Osteosarcoma of distal femur.</p> <p><b>MRI of the distal femur:</b></p> <ul style="list-style-type: none"> <li>mixed intensity mass lesion involving the distal end of femur involving the meta-diaphysis, extension into the epiphysis, with intact articular margin of the femur and trans cortical and periosteal extension of the soft tissue.</li> <li>Extra-osseous extension of the mass lesion is seen into the overlying soft tissue and posteriorly the lesion is extending into the knee joint (Fig. 4A).</li> <li>MRI scans also revealed a focal T2 hyperintense lesion in proximal shaft of femur, skip lesion.</li> </ul> <p><b>Isotope scanning:</b></p> <ul style="list-style-type: none"> <li>diffuse uptake in the lesion with no significant uptake in lesion in proximal femoral shaft.</li> </ul> <p><b>AP and lateral X rays</b> of the forearm</p> <ul style="list-style-type: none"> <li>diaphyseal lesion along external surface of lower humeral shaft with saucerization of the cortex, and new bone formation within the soft tissue and radiolucent mass extending into surrounding soft tissue. There is cortical thickening with Codman's triangle seen at margin of the lesion (Fig. 5A).</li> </ul> <p><b>Diagnosis:</b> Possibility of agsive lesion ; parosteal variety of osteosarcoma. Differential diagnosis: myositis ossificans in view of history of trauma.</p> <p><b>MRI:</b></p> <ul style="list-style-type: none"> <li>heterogeneously enhancing soft tissue mass on surface of lower humerus showing dense areas of peripheral blooming representing new bone formation. No intramedullary invasion could be seen and erosion and saucerization of cortex.</li> <li>DWI images reveal diffusion restriction with ADC reversal of the lesion (Fig. 5A).</li> </ul> <p><b>CT Scan:</b></p> <ul style="list-style-type: none"> <li>confirmed cortical involvement with saucerization and dense mineralization in the soft tissue component. Periosteal reaction seen on the surface of bone.</li> <li>CT guided biopsy was performed to establish a definitive diagnosis (Fig. 5A).</li> </ul> <p><b>CT scan:</b></p> <ul style="list-style-type: none"> <li>thickening of the walls of maxillary sinus with osseous soft tissue mass and sunray type of ossification and periosteal reaction, obliterating the air space (Fig. 6A).</li> <li>extension of the ossified soft tissue into the nasal cavity and floor of the mouth.</li> </ul> <p><b>Diagnosis:</b> aggressive bone forming tumor: osteosarcoma.</p> <p><b>Chest X-Ray:</b> revealed few calcified nodular lesions in both lungs (Fig. 6A).</p> <p><b>CT chest:</b> confirmed the calcified nodules and also revealed a well-defined lytic lesion in D8 vertebra.</p> <p><b>MRI of the dorso-lumbar spine:</b></p> <ul style="list-style-type: none"> <li>marrow infiltration of D8 vertebra and left sided posterior elements by enhancing soft tissue mass lesion with extra osseous extension of the soft tissue in adjacent muscles involving costovertebral junction (Fig. 6B).</li> </ul> <p><b>CT guided biopsy</b> from this lesion (Fig. 6B) was done .</p> <p><b>X-ray</b> of the humerus:</p> <ul style="list-style-type: none"> <li>a large expansile lytic lesion in proximal shaft of the left humerus with ill-defined margins and broad zone of transition.</li> <li>Multiple internal septations were seen with thinning and irregularity of overlying cortex.</li> <li>Few subtle foci of calcifications were seen within the lesion (Fig. 7).</li> </ul>	<b>Biopsy:</b> <ul style="list-style-type: none"> <li>histopathology revealed predominantly osteoblastic cells with enhanced nucleocytoplasmic ratio and undifferentiation: high-grade osteosarcoma (Fig. 4B).</li> </ul> <p><b>Treatment:</b></p> <ul style="list-style-type: none"> <li>Chemotherapy followed by surgical excision with negative surgical margins of the excised tumor.</li> <li>Wide resection and reconstruction by endoprosthesis and knee joint replacement was done and follow up check radiograph (Fig. 4B).</li> </ul> <p><b>Histopathology:</b> osteoblastic activity representing intermediate to high-grade osteosarcoma with extensive bone matrix and small amount of fibroblastic cellular atypia.</p> <p><b>Histopathology (D8):</b> high grade metastatic osteoblastic cells with proliferation of spindle cells, atypical chondrocytes and neo-osteogenesis, metastasis from high grade osteosarcoma.</p> <p><b>Treatment:</b></p> <ul style="list-style-type: none"> <li>Neoadjuvant chemotherapy</li> <li>Follow up scan revealed a mild regression in calcified nodular metastasis to the lungs and also there was regression in soft tissue associated with vertebral metastasis</li> </ul> <p><b>Biopsy:</b></p> <ul style="list-style-type: none"> <li>cartilaginous component with poorly differentiated and high cellular atypia confirming Chondrosarcoma.</li> </ul> <p><b>Treatment:</b> Wide resection and reconstruction by endoprosthesis was performed followed by chemotherapy (Fig. 7).</p>
5.	13 year girl presented with gradual increasing painless swelling over distal arm. She is a kabaddi player and got hit during a kabaddi match. <b>Examination</b> revealed a hard swelling along the anterior aspect of arm proximal to elbow joint. AP and lateral X-ray of arm are advised.		
6.	A 25-year male swelling in the upper jaw region swelling started intraorally and gradually increased in size. It was associated with difficulty in opening of the mouth and pain on palpation. CT scan of the face and sinuses was advised.		
7.	40 years male: pain and discomfort in left upper arm.		

(continued on next page)

Table 1 (continued)

Case	Clinical	Imaging	Management
		<p><b>Diagnosis:</b> Features were consistent with aggressive bone lesion with possibility of chondroid origin.</p> <p><b>MRI:</b></p> <ul style="list-style-type: none"> <li>diffuse highly hyperintense signal mass lesion representing medullary calcific lobules and punctate low signal intensity foci representing medullary calcifications: chondroid matrix (Fig. 7).</li> </ul>	
8.	<p>A 28-year-old female patient presented with increasing swelling and pain in right ring finger.</p> <p><b>Examination</b> the swelling was localized to proximal aspect of the finger and movement at metacarpophalangeal joint</p>	<p><b>X-ray</b> of the index finger:</p> <ul style="list-style-type: none"> <li>large lytic lesion with few septations and thinning of the overlying cortex in proximal shaft of proximal phalanx of index finger extending up to the articular surface with well-defined margins.</li> <li>narrow zone of transition.</li> <li>No definite matrix mineralization or obvious cortical break could be delineated (Fig. 8A).</li> </ul> <p><b>Diagnosis:</b> Findings were in favor of nonaggressive lesion with possibilities of GCT or enchondroma.</p> <p><b>MRI</b> of the finger:</p> <ul style="list-style-type: none"> <li>confirmed a large heterogeneous soft tissue lesion in the corresponding location with partial resorption of overlying cortex.</li> <li>DWI images reveal restricted diffusion with reversal of signal on ADC (Fig. 8A).</li> </ul>	<p><b>Treatment:</b> Surgery with bone graft was placed within the bone defect created postoperatively (Fig. 8B).</p> <p><b>Histopathology:</b> multinucleated giant cells without evidence of malignant transformation: low grade Giant cell tumor.</p>
9.	<p>20 years old male patient presented with severe pain in right lower leg, and relieved by salicylates. Associated history of fever or malaise was absent.</p>	<p><b>AP and lateral X rays</b> of the lower leg</p> <ul style="list-style-type: none"> <li>focal cortical thickening along anterior and medial cortex of mid shaft of tibia (Fig. 9).</li> </ul> <p><b>Diagnosis:</b> Possibility of Osteoid Osteoma</p> <p><b>MRI:</b></p> <ul style="list-style-type: none"> <li>Axial T2-weighted MR images shows the nidus, with diffuse cortical thickening and there is edema in the surrounding bone marrow and soft tissue (Fig. 9).</li> </ul> <p><b>Nuclear scan:</b></p> <ul style="list-style-type: none"> <li>Intense uptake at the site of lesion confirming the nidus (Fig. 9).</li> </ul>	<p><b>Treatment:</b> Local excision of the cortex containing the tumor</p> <p><b>Histopathology:</b></p> <ul style="list-style-type: none"> <li>to confirm complete removal of nidus.</li> <li>Postoperative X-rays were obtained to confirm the complete removal (Fig. 9) and patient eventually was completely pain free.</li> </ul>
10.	<p>16 years female pain in right arm. No associated history of fever was elicited.</p>	<p><b>AP and lateral X rays</b> of the arm:</p> <ul style="list-style-type: none"> <li>a large eccentric expansile lytic lesion in proximal shaft of humerus involving metadiaphysis with well-defined margin and narrow zone of transition and thinning of overlying cortex.</li> <li>No matrix mineralization appreciated on plain X-ray. No obvious periosteal reaction or cortical break (Fig. 10).</li> </ul> <p><b>Diagnosis:</b> features of benign bony lesion with possibility of simple bony cyst/fibrous dysplasia.</p> <p><b>MRI:</b></p> <ul style="list-style-type: none"> <li>a well-defined fluid intensity lesion in proximal metadiaphysis of humerus. No evidence of heterogeneous signal or fluid - fluid level seen ruling out internal hemorrhage (Fig. 10).</li> </ul>	<p><b>Treatment:</b> surgery with bony curettage and bone grafting.</p>
11.	<p>27 year female had a chest X-ray done for cough.</p>	<p><b>Chest X-Ray:</b> Lungs were clear with clear costophrenic angles. However a dense expansile lesion seen in lateral aspect of left 6th rib (Fig. 11).</p> <p><b>CT scan</b> An expansile lytic lesion in left 6th rib with thick sclerotic margins and central ground glass haziness consistent No associated soft tissue changes were seen (Fig. 11).</p>	
12.	<p>26 years boy: palpable hard swelling below the knee joint.</p>	<p><b>Radiological diagnosis:</b> Fibrous Dysplasia.</p> <p><b>X-ray</b> of knee:</p> <ul style="list-style-type: none"> <li>An osteochondral outgrowth from the anterior aspect of proximal tibia. There is continuity of the lesion with the medullary cavity representing osteochondroma (Fig. 12).</li> </ul> <p><b>MRI</b></p> <ul style="list-style-type: none"> <li>Confirm the thickness of cartilaginous cap and changes in adjacent soft tissue (Fig. 12).</li> </ul>	

**Table 2**

Staging of malignant bone tumors : defined by AJCC in 1983 and revised in 2003.

Stage	Tumour	Lymph node	Metastasis	Grade
IA	T1	N0	M0	G1 or G2
IB	T2	N0	M0	G1 or G2
IIA	T1	N0	M0	G3 or G4
IIB	T2	N0	M0	G3 or G4
III	T3	N0	M0	Any G
IVA	Any T	N0	M1a	Any G
IVB	Any T	N1	Any M	Any G
IVB	Any T	Any N	M1b	Any G

The extent of tumour (T), T1 = tumor size 8 cm or less, T2 = tumor length 8 cm or above. T3 = indicates skip lesions.

Nodal status (N), N0 = no loco-regional lymph node enlargement, N1 = loco-regional metastasis.

Metastasis (M), M0 = absence of distant metastasis, M1a = metastasis to lungs M1b = metastasis to other sites.

Histology grade of the tumour (G), G1 = Low grade/well differentiated, G2 = Moderately differentiated, G3 = high grade/poorly differentiated, G4 = undifferentiated.

Classification/staging of malignant tumours has been defined by AJCC in 1983 and revised in 2003,<sup>22</sup>: Table 2.

#### 4. Conclusion

With availability of wide range of imaging options, appropriate selection of imaging modality is one of the most important steps in patients with bone tumor. Imaging studies plays crucial role in the disease detection, precise diagnosis, treatment planning and post-treatment surveillance in these patients, as illustrated in these cases.

It is crucial to understand that though CT/MR imaging offers excellent delineation of the osseous and musculoskeletal structures, conventional radiograph remains the most important investigation for the primary diagnosis of bone tumor. Excellent soft tissue resolution of MRI helps in precise delineation of the extent of marrow and soft tissue involvement and is therefore the best modality for local staging. Further advances in imaging with state of art MRI techniques like DWI and Dynamic contrast scans helps in assessing post-treatment response. PET-CT/PET-MRI along with nuclear scanning is more appropriate investigations for overall staging of the disease because of their capability to detect skip lesions and distant metastasis. High spacial resolution of CT makes it the best option for image-guided biopsies. Multi-planer capabilities of CT/MRI help in precise pre-operative localization of the lesion. Moreover, multi-disciplinary approach is vital in these patients with bone tumor to ensure efficient disease diagnosis and best treatment responses.

#### Conflicts of interest

None of the authors have any conflicts of interest or financial ties to disclose.

#### Appendix A. Supplementary data

Supplementary data to this article can be found online at

<https://doi.org/10.1016/j.jcot.2019.05.022>.

#### References

- Berquist TH, Dalinka MK, Alazraki N, et al. Bone tumors: American College of Radiology—ACR appropriateness criteria. *Radiology*. 2000;215(suppl):261–264.
- Costelloe CM, Rohren EM, Madewell JE, et al. Imaging bone metastases in breast cancer: techniques and recommendations for diagnosis. *Lancet Oncol*. 2009;10:606–614.
- Miller TT. Bone tumors and tumor-like conditions: analysis with conventional radiography. *Radiology*. 2008;246(3):662–674.
- Costelloe Colleen M, Madewell John E. Radiography in the initial diagnosis of primary bone tumors. *AJR*. 2013;200:3–7.
- Zampa Virma, Giuliana R, et al. MRI of bone tumors: advances in diagnosis and treatment assessment. *Imaging Med*. 2010;2(3):325–340.
- Salamipour H, Jimenez RM, Brec SL, Chapman VM, Kalra MK, Jaramillo D. Multidetector row CT in pediatric musculoskeletal imaging. *Pediatr Radiol*. 2005;35:555–564.
- love Charito, Din Anabella S, et al. Radionuclide bone imaging: an illustrative review. *Radiographics*. 2003;23:341–348.
- Ardran GM. Bone destruction not demonstrable by radiography. *Br J Radiol*. 1951;24:107–109.
- Morrison WB, Dalinka MK, Daffner RH, et al. *Bone tumors. ACR Appropriateness Criteria*. Reston, VA: American College of Radiology; 2005:1–5.
- Costelloe Colleen M, Chuang Hubert H, et al. FDG PET/CT of primary bone tumors. *AJR*. 2014;202:W521–W531.
- Schulte M, Brecht-Krauss D, Heymer B, et al. Grading of tumors and tumorlike lesions of bone: evaluation by FDG PET. *J Nucl Med*. 2000;41:1695–1701.
- Dimitrakopoulou-Strauss A, Strauss LG, Heichel T, et al. The role of quantitative <sup>18</sup>F-FDG PET studies for the differentiation of malignant and benign bone lesions. *J Nucl Med*. 2002;43:510–518.
- Kong CB, Byun BH, Lim I, et al. <sup>18</sup>F-FDG PET SUVmax as an indicator of histopathologic response after neoadjuvant chemotherapy in extremity osteosarcoma. *Eur J Nucl Med Mol Imaging*. 2013;40:728–736.
- Catana C, Guimaraes AR, Rosen BR. PET and MR imaging: the odd couple or a match made in heaven? *J Nucl Med*. 2013;54:815–824.
- Stacy Gregory S, Mahal Ravinder S, et al. Staging of bone tumors: a review with illustrative examples. *AJR*. 2006;186:967–976.
- Madewell JE, Ragsdale BD, Sweet DE. Radiologic and pathologic analysis of solitary bone lesions. Part I. Internal margins. *Radiol Clin*. 1981;19:715–748.
- Lodwick GS, Wilson AJ, Farrell C, Virtama P, Dittich F. Determining growth rates of focal lesions of bone from radiographs. *Radiology*. 1980;134:577–583.
- Oudenhoven LF, Dhondt E, Kahn S, et al. Accuracy of radiography in grading and tissue-specific diagnosis: a study of 200 consecutive bone tumors of the hand. *Skeletal Radiol*. 2006;35:78–87.
- Sweet DE, Madewell JE, Ragsdale BD. Radiologic and pathologic analysis of solitary bone lesions. Part III. Matrix patterns. *Radiol Clin*. 1981;19:785–814.
- Ragsdale BD, Madewell JE, Sweet DE. Radiologic and pathologic analysis of solitary bone lesions. Part II. Periosteal reactions. *Radiol Clin*. 1981;19:749–783.
- Enneking WF. Staging musculoskeletal tumors. In: Enneking WF, ed. *Musculoskeletal Tumor Surgery*. New York, NY: Churchill Livingstone; 1983:87–88.
- American joint committee on cancer. Bone. In: Greene FL, Page DL, Fleming ID, et al., eds. *AJCC Cancer Staging Manual*. New York, NY: Springer-Verlag; 2002:213–219.
- Van Rijswijk CS, Geirnaerd MJ, Hogendoorn PC, et al. Soft-tissue tumors: value of static and dynamic gadopentetate dimeglumine-enhanced MR imaging in prediction of malignancy. *Radiology*. 2004;233(2):493–502.
- Tokuda O, Hayashi N, Taguchi K, et al. Dynamic contrast-enhanced perfusion MR imaging of diseased vertebrae: analysis of three parameters and the distribution of the time-intensity curve patterns. *Skeletal Radiol*. 2005;34(10):632–638.
- Kajihara M, Sugawara Y, Sakayama K, et al. Evaluation of tumor blood flow in musculoskeletal lesions: dynamic contrast-enhanced MR imaging and its possibility when monitoring the response to preoperative chemotherapy-work in progress. *Radiat Med*. 2007;25(3):94–105.
- Costa FM, Ferreira EC, Vianna EM. Diffusion-weighted magnetic resonance imaging for the evaluation of musculoskeletal tumors. *Magn Reson Imag Clin N Am*. 2011;19(1):159–180.
- Van Rijswijk CS, Kunz P, Hogendoorn PC, et al. Diffusion-weighted MRI in the characterization of soft-tissue tumors. *J Magn Reson Imaging*. 2002;15(3):302–307.